

Crankshaft geometry modification and strength simulations for a new design of diesel opposed-piston engine

ARTICLE INFO

Received: 31 May 2023
Revised: 6 July 2023
Accepted: 7 July 2023
Available online: 8 August 2023

The article presents simulation strength calculations of a newly designed crankshaft for a PZL 100 engine with a reciprocating piston design. This engine is the subject of a research and development project co-financed by NCBR. The article presents four successive versions of the crankshaft geometric changes which underwent strength calculations. Such elements as the outer and inner parts of the crankshaft arm were changed in these geometric versions. The geometry of the shaft was changed using Catia v5 software, while strength calculations were carried out in Abaqus software. In summary, one of the presented models was selected for further work due to the possible simplification of the manufacturing process and the reduction of mass and stresses. This model was further investigated in the project.

Key words: crankshaft, FEM, diesel, opposed-piston engine, strength

This is an open access article under the CC BY license (<http://creativecommons.org/licenses/by/4.0/>)

1. Introduction

The crankshaft is one of the main components of an internal combustion engine. Its task is to convert reciprocating motion into rotary motion. Crankshafts in internal combustion engines are subjected to high load indirectly resulting from piston force. In most cases, research into crankshaft strength is limited to checking crankshaft wear resistance to bending and twisting conditions. Increasingly, simulation tools based on FEM analysis are being used for such calculations. [19]. This approach saves time during the pro-design of a new engine structural component such as the crankshaft.

The authors of the article used computer-aided design software and wear resistance simulation software to study the effect of changing the external geometry of the crankshaft on its strength. It should be noted that the geometric solutions presented in the article are new designs, and the crankshaft itself was subjected to a design process for the new PZL-100 aircraft diesel engine developed by WSK "PZL-Kalisz" S.A. The goal of the project was to develop a two-stroke supercharged diesel engine for aircraft propulsion. The engine will feature reduced unit weight, fuel consumption and CO₂ emissions thanks to supercharging, a uniflow charge exchange system and direct fuel injection into the central combustion chamber. This will result in shorter combustion times, reduced heat loss and high efficiency. The two-stroke nature of the operation, increased speed (no valvetrain) and increased supercharging will increase specific power compared to current aircraft engines. Aircraft diesel engines including opposed piston engines were analyzed in [7]. Opposed piston engines are currently in use, for example the Achates Power engine for powering trucks and military vehicles [15, 18].

If you look more closely at the market, you can notice that the main competing solutions that exist on the drawing board include such engine designs as Motors Rotax 912 and 914 (BRP-Powertrain GmbH & Co KG), Lycoming O-235 (Lycoming Engines) or Continental O-200 (Continental Motors, Inc.). It should be added that the Rotax 912 engine

is used in the majority of manufactured windjammers. Similarly, the ultralight recreational aircraft market commonly used a Rotax engine that allows refueling with standard automotive gasoline. Another competitive solution is the Avco Lycoming O-235 engine which belongs to a family of air-cooled four-cylinder aircraft engines. Similar engines are offered by Continental. In summary, the engine under design is expected to provide power and weight at the level of competing engines, with a reduction in operating costs and CO₂ emissions due to Diesel fuel.

The engineering design process of the crankshaft consisted in developing a new crankshaft geometry for an aircraft diesel engine with opposite pistons. Thus, the design process was a multi-stage one, and the presented article contains a description of part of the work carried out under the project. The work on the above-mentioned engine also included issues related to the construction of the piston [17] or modeling of dynamic phenomena [9]. It is worth mentioning that earlier geometric versions of the designed crankshaft were subjected to both strength calculations and checking their natural frequency [8]. There are also publications examining opposite piston engines in terms of the thermodynamic process [20] or numerical analysis of the impact of crank mechanism design on engine efficiency [16].

The results of the simulation studies presented in the article are the same as those currently being conducted all over the world. Similar research issues include the methodology of testing in ANSYS [21] or the effect of changing the crankshaft material on its strength [11]. There are also publications whose authors use the same simulation software as in this article. The authors of the publication [12] presented a comprehensive approach to the influence of dynamic loads calculated in Adams and load-bearing loads in Abaqus. An equally important issue currently under study is strength analysis for residual stress during shaft bending [4, 5]. In addition to strength analysis, some of the works preface a comprehensive approach to fatigue life analysis and the evaluation of crankshaft life [3] or analyze the cause of critical shaft damage [2, 23]. The above publi-

cations indicate that preliminary strength calculations of the new crankshaft to estimate its strength are therefore crucial.

2. Model description

The geometry of the shaft was prepared using Catia v5 software which is commonly used for such a design of crankshaft geometry [22], while strength calculations were carried out in Abaqus software. The finite element method that was used is one of the most effective and widely used numerical methods, based on the discretization of a continuous model.

Using the FEM, we can consider the process of approximating a continuous medium (real object), having an infinite number of degrees of freedom, with a set of sub-areas (discrete model) and a finite number of degrees of freedom. The calculations that have been performed in Abaqus use the incremental method combined with iterative algorithms or the so-called Newton-Raphson (NR) method. It is the most typical incremental-iterative algorithm used in displacement methods, giving accurate results and ensuring rapid convergence in most cases encountered in practice in structural mechanics.

Each change in geometry was analyzed in terms of balancing the rotating masses, which is extremely significant for the crankshaft of the two-stroke engine [14]. The basic design assumptions of the crankshaft were mostly directly derived from the geometry of the newly developed engine which specifies that the shaft should have three cranks offset from each other successively by an angle of 120° with 100 mm spacing along the axis of rotation. In addition, the radius of the crank should provide 72 mm of piston travel. Only the central section of the crankshaft which is exposed to the highest external forces was subjected to strength testing. This is because the central section of the crankshaft is exposed to the maximum values of forces. For all four simulation cases, the same (verified) design mesh density was established with a single element size of 1.1 mm. Before the original simulation, the size of the mesh was checked with the pre-simulation studies. It was proven that a mesh smaller than 1.1 mm would give no significant changes in the results. Consequently, it was decided not to make the mesh dense at any part of the model. Normally, if the mesh size is not correct, you should making the mesh dense in critical spots of geometry as presented in [13].

All models presented were calculated for two conditions, i.e. bending and twisting. The force loading conditions were implemented from the previous simulation calculations performed in MCS Adams. According to the earlier calculations, the highest piston force acting on the crankshaft occurs for the values of 0 CAD and 14.5 CAD, as shown schematically in Fig. 1. The same method was used by the authors of [12] who determined the maximum forces for bending and twisting.

A material for the crankshaft defined as cast iron was assumed for the simulation calculations. The material properties adopted for the calculations are shown in Table 1.

The conditions of immobilization at one side and the possibility of free rotation on the other side were imposed on the crankshaft. Additionally, to reflect the restraint conditions, it was decided to immobilize the crankshaft by using an intermediate element as a bushing. Otherwise,

when restraining directly the surfaces the shaft was supported on, local maximum stresses occurred. This happened because high stresses were created at the edge between the restrained and moving surfaces, resulting mainly from the local shear stresses. Such a situation does not occur when the crankshaft operates in an internal combustion engine, so it was decided to immobilize the crankshaft by an intermediate element, i.e. a bushing. Additional elements like bushings imposed the need to define the contact conditions between the crankshaft and additional bushings. These conditions were defined as "normal contact", which reflects the contact of components across their entire surface. The bushings were made of 40H steel whose properties are specified in Table 1.

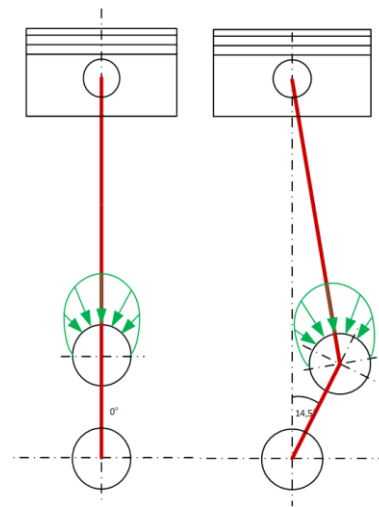


Fig. 1. Boundary conditions as forces acting on the model

Table 1. Material properties adopted for the calculation

Properties	Crankshaft	Bushing
Poisson's number	0.3	0.3
Density	7197 kg/m ³	7850 kg/m ³
Young's modulus	178 GPa	207 GPa

3. Geometry change in models 1–4

3.1. Geometry of model 1

The geometry of the crankshaft developed for the research engine was designed based on the analyzed literature [6] and the design solutions used in modern OPOS engines. The basic design assumptions of the crankshaft are mostly directly derived from the geometry of the newly developed engine which was initially described in the first section of this article. In addition, it was also assumed that the shaft at the air intake side will be made similarly to the crankshaft at the exhaust side although it carries lower loads. The solid model shown in Fig. 3 shows a crankshaft designed along the lines of the crankshaft of the Gemini 100 engine (Fig. 2) and follows the above guidelines.

3.2. Geometry of model 2

The second geometric model of the crankshaft was slightly modified in relation to the first model. The outer part of the crankshaft arm was modified by introducing an undercut with a radius of 60 mm instead of the rounding with a radius of 220 mm, mainly aimed at conducting strength tests with reduced mass.



Fig. 2. View of the Gemini 100 engine crankshaft [1]

3.3. Geometry of model 3

The third geometric model of the crankshaft analogous to model 2 has reduced weight. This time, however, it was less than 5 kg. This was only possible by modifying the inner part of the crankshaft arm by introducing an undercut with a radius of 60 mm in place of the 220 mm radius rounding. The project was mainly aimed at carrying out strength analysis of the crankshaft structure at the maximum reduced weight.

3.4. Geometry of model 4

The fourth geometric model of the crankshaft, unlike the previous versions, was designed to simplify the structure as much as possible. To this end, the geometries forming the outer and inner shapes of the radial arms were replaced by straight sections equidistant from each other. This will reduce their manufacturing time and the manner of the complexity of the machining process of the crankshaft. A beneficial aspect of the modification is the fact that the weight of the component is reduced compared to the first model.

The changes in the geometry of a single crankshaft compared to previous models are presented in Table 2 (the changes are marked in orange).

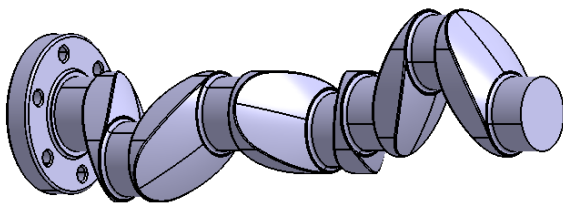


Fig. 3. Geometry of model 1

4. Results

The results present 4 geometrical models of the crankshaft. The results are grouped into 4 groups to sequentially represent the results of the bending and twisting strength calculations. In each model, the results of the strength tests were presented as stress maps on the external surface of the shafts during both the bending and twisting simulations. In addition, the mass of the entire crankshaft was calculated for each case. All the presented results refer to the identical range from 0 to 120 MPa so they can be compared.

Table 2. Geometry compared to model 1

Model number	Geometry view
1	
2	
3	
4	

4.1. Bending results in model 1-4

As can be seen in the figures below, the highest stresses occur at the rounded point between the surface of the crankshaft and the side surface of the counterweight. The maximum values that occur there were observed for model 3 and reached 122.9 MPa, while the lowest stress concentration was observed for model 4 and reached 107.8 MPa. The results for all models are compared in Table 3 and Fig. 4. On the other hand, at the center of the bottom surface of the crankshaft, the maximum stresses vary between 60–70 MPa for models 1, 2 and 4 and 70–80 MPa for model 3.

However, it should be noted that the stress distribution in the crankshaft section is uniform and shows a typical distribution for bending.

The stress distributions are symmetrical with respect to the connecting rod placement because of to the symmetrical load on both sides of the crankshaft.

The influence of the crankshaft geometry on the distribution of stresses is well shown in Table 3. The zone of stress concentration on the side surfaces of the crankshafts is the larger, the smaller the cross-section of the crankshaft is.

4.2. Twisting results in model 1-4

The figures show that the highest stresses are at the rounded point between the surface of the main bearings and the side surface of the counterweight, particularly on the left. This is the side where the crankshaft surface was immobilized for the direction of movement along the main axis of the crankshaft. The maximum values that occur there were observed for model 3 and reached 132.7 MPa, while the lowest stress concentration, i.e. 126.8 MPa was observed for model 2. The results for all models are compared in Table 4 and Fig. 4. On the other hand, at the center of the bottom surface of the crankshaft, the maximum stresses vary between 70–80 MPa for models 1 and 2 and 60–70 MPa for models 3 and 4.

However, it should be noted that the distribution of stresses in the crankshaft section is uniform and shows a typical distribution for twisting. The stress distributions are almost symmetrical concerning the connecting rod bearing, however, it is clear that the left crankshaft arm is subjected to greater stress than the right one. This is due to the accumulation of torque on this crank.

5. Discussion of the results

The maximum stresses that occurred in all models during bending and torsion simulations are compared Table 5 and Fig. 4. Different types of support for the crankshaft during the simulations enable us to compare the values of the maximum stresses in all models. In addition, the table presents the mass of the entire crankshaft. The mass was calculated from the density of the material used.

The data in the table show that each version of the crankshaft has its positive and negative aspects. It is worth mentioning that the maximum stress for bending and twisting does not exceed 135 MPa, which can be considered an acceptable value for the material used. For comparison purposes, the authors of a similar solution obtained values above 300 MPa in dynamic tests [10]. In this research, dynamic loads were not analyzed as this was not the final geometric version of the crankshaft.

To sum up, model 1 has a reduced mass but increased stresses for bending and compression. Model 2, despite its reduced mass, has reduced stresses compared to its predecessor. Model 3 has the lowest mass but shows the highest bending stresses. Model 4 has a mass comparable to its predecessors, its bending stresses are low, and its compressive stresses are medium. The authors conclude that model 4 should be selected for further work due to a possible simplification of its manufacturing process and the reduction of its mass and stresses. This model was further studied in the project.

Table 3. Stress simulation results for bending

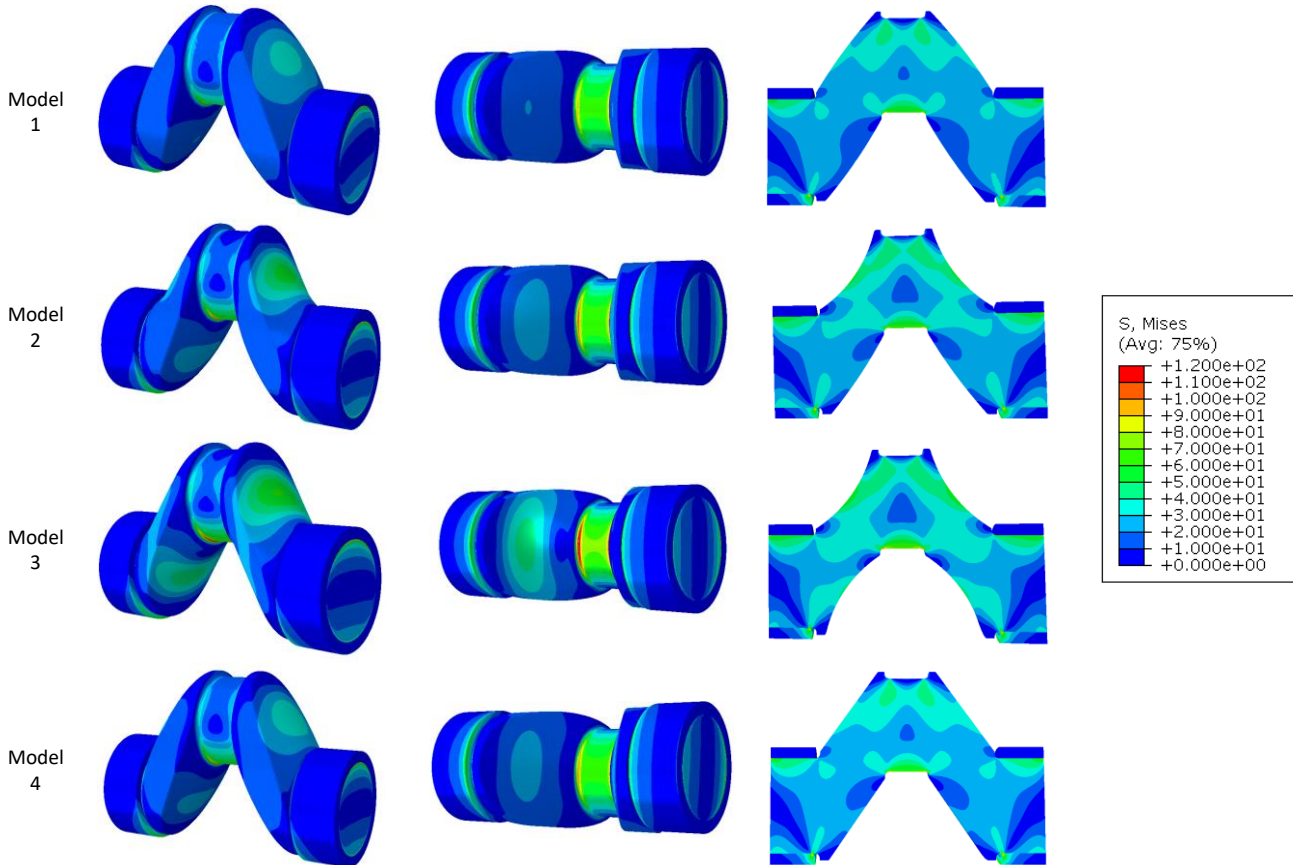


Table 4. Stress simulation results for twisting

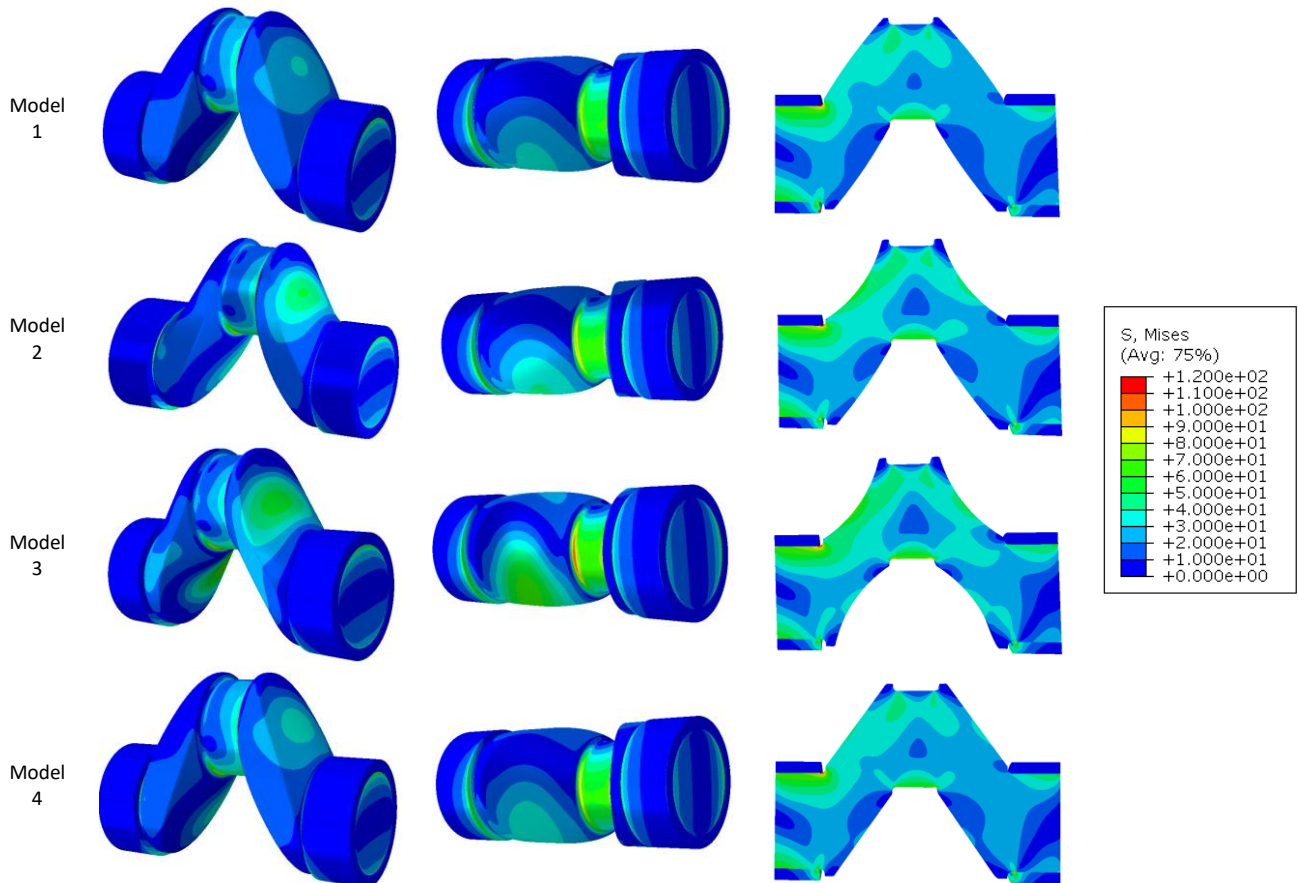


Table 5. Stress for bending and twisting

Model number	Bending [MPa]	Twisting [MPa]	Mass of crankshaft [kg]
Model 1	119.2	128.6	5.65
Model 2	113.7	126.8	5.30
Model 3	122.9	132.2	4.94
Model 4	107.8	132.4	5.53

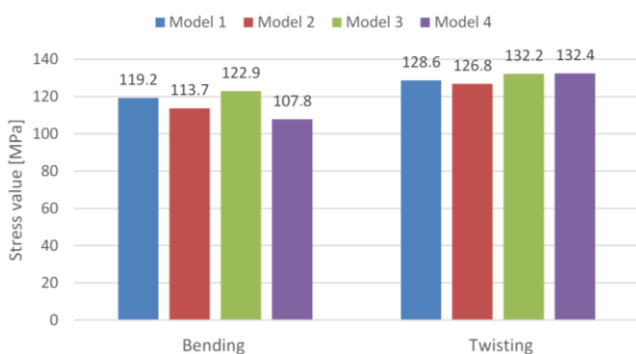


Fig. 4. Stress for bending and twisting

6. Conclusions

The conclusions that can be drawn from the presented results are as follows:

- modern design and simulation methods allow for improving the design of processors of crankshafts of internal combustion engines
- at the stage of designing new engine elements, it is possible to assess the strength of a given part
- the authors of this paper analyzed the strength of four different geometric versions of the crankshaft and selected the model for further design work
- the same material was adopted in all models, but its change can affect strength
- the material density and volume of the geometric model of the crankshaft enabled us to estimate its mass, which also influenced the selection of the target model for further work because the designed crankshaft will potentially be used in an aircraft engine
- the conducted research is part of the worldwide trend of using modern simulation methods for fatigue calculations of engine parts.

Acknowledgements

This work has been realized in cooperation with The Construction Office of WSK "PZL-KALISZ" S.A." and is part of Grant Agreement No. POIR.01.02.00-00-0002/15 financed by the Polish National Centre for Research and Development.

Nomenclature

CAD	crank angle degree	OPOS	opposed-piston
FEM	finite element method	PZL	Polskie Zakłady Lotnicze
NCBR	Polish National Centre for Research and Development	WSK	Wytwórnia Sprzętu Komunikacyjnego

Bibliography

- [1] Anderson T. Superior's New Gemini Diesel (posted on 28.06.2015). <http://www.dieselarmy.com/news/video-superiors-new-gemini-diesel/>
- [2] Ang YZ, Ku PX. Study on failure analysis of crankshaft using finite element analysis. MATEC Web Conf. 2021;335: 03001. <https://doi.org/10.1051/mateconf/202133503001>
- [3] Bulut M, Cihan O, Temizer I. Fatigue life and stress analysis of the crankshaft of a single cylinder diesel engine under variable forces and speeds. Mater Test. 2021;63(8):770-777. <https://doi.org/10.1515/mt-2020-0122>
- [4] Chien WY, Pan J, Close D, Ho S. Fatigue analysis of crankshaft sections under bending with consideration of residual stresses. Int J Fatigue. 2005;1(27):1-19. <https://doi.org/10.1016/j.ijfatigue.2004.06.009>
- [5] Choi KS, Pan J. Simulations of stress distributions in crankshaft sections under fillet rolling and bending fatigue tests. Int J Fatigue. 2009;31(3):544-557. <https://doi.org/10.1016/j.ijfatigue.2008.03.035>
- [6] Flint M, Pirault J-P. Opposed piston engines: evolution, use, and future applications. SAE International 2009.
- [7] Gęca M, Czyz Z, Sulek M. Diesel engine for aircraft propulsion system. Combustion Engines. 2017;169(2):7-13. <https://doi.org/10.19206/CE-2017-202>
- [8] Grabowski Ł, Pietrykowski K, Karpiński P. FEM simulation research of natural frequency vibration of crankshaft from internal combustion engine. ITM Web Conf. 2017;15: 07004. <https://doi.org/10.1051/itmconf/20171507004>
- [9] Grabowski Ł, Pietrykowski K, Karpiński P. The zero-dimensional model of the scavenging process in the opposed-piston two-stroke aircraft diesel engine. Propulsion and Power Research. 2019;8(4):300-309. <https://doi.org/10.1016/j.jprr.2019.11.003>
- [10] He CM, Xu SC. Opposed-piston crankshaft system dynamics simulation and durability analysis in a neotype two-stroke diesel engine. American Journal of Mechanical and Industrial Engineering. 2017;2(2):54-63. <https://doi.org/10.11648/j.ajmie.20170202.11>
- [11] Karthick L, Stephen Leon J, Ravi R, Michel J, Mallireddy N, Vadivukarasi L. Modelling and analysis of an EN8 crankshaft in comparison with AISI 4130 crankshaft material. Mater Today-Proc. 2022;52(3):1036-1040. <https://doi.org/10.1016/j.matpr.2021.10.484>
- [12] Montazersadgh FH, Fatemi A. Dynamic load and stress analysis of a crankshaft. SAE Technical Paper 2007-01-0258. 2007. <https://doi.org/10.4271/2007-01-0258>
- [13] Montazersadgh FH, Fatemi A. Stress analysis and optimization of crankshafts subject to dynamic loading. A Final Project Report Submitted to the Forging Industry Educational Research Foundation (FIERF) and American Iron and Steel Institute (AISI). 2007.
- [14] Mosakowski R. Analysis of balancing of six-cylinder in-line two-stroke internal combustion engines. Combustion Engines. 2009;139(4):22-33. <https://doi.org/10.19206/CE-117165>
- [15] Naik S, Johnson D, Fromm L, Koszewnik J, Redon F, Regner G et al. Achieving Bharat Stage VI emissions regulations while improving fuel economy with the opposed-piston engine. SAE Int J Engines. 2017;10(1):17-26. <https://doi.org/10.4271/2017-26-0056>
- [16] Opaliński M, Teodorczyk A, Kalke J. The closed-cycle model numerical analysis of the impact of crank mechanism design on engine efficiency. Combustion Engines. 2017; 168(1):153-160. <https://doi.org/10.19206/CE-2017-125>
- [17] Pietrykowski K, Magryta P, Skiba K. Finite element analysis of a composite piston for a diesel aircraft engine. Combustion Engines. 2019;179(4):107-111. <https://doi.org/10.19206/CE-2019-417>
- [18] Regner G, Johnson D, Koszewnik J, Dion E, Redon F, Fromm L. Modernizing the opposed piston, two stroke engine for clean, efficient transportation. SAE Technical Paper 2013-26-0114. 2013. <https://doi.org/10.4271/2013-26-0114>
- [19] Sandya K, Keerthi M, Srinivas K. Modeling and stress analysis of crankshaft using FEM package Ansys. International Research Journal of Engineering and Technology. 2016;3(1):687-693. <https://www.irjet.net/archives/V3/i1/IRJET-V3I1119.pdf>
- [20] Shokrollahihassanbarough F, Alqahtani A, Wyszynski ML. Thermodynamic simulation comparison of opposed two-stroke and conventional four-stroke engines. Combustion Engines. 2015;162(3):78-84. <https://doi.org/10.19206/CE-116867>
- [21] Thejasree P, Dileep Kumar G, Leela Prasanna Lakshmi S. Modelling and analysis of crankshaft for passenger car using ANSYS. Mater Today-Proc. 2017;4(10):11292-11299. <https://doi.org/10.1016/j.matpr.2017.09.053>
- [22] Vinay AV, Shankar MU, Satya LP, Kumar YS, Srikanth M. Modelling and analysis of crankshaft for four stroke diesel engine by using composite materials. Bachelor Thesis in Anil Neerukonda Institute of Technology and Sciences. India 2021.
- [23] Witek L, Sikora M, Stachowicz F, Trzepiecinski T. Stress and failure analysis of the crankshaft of diesel engine. Eng Fail Anal. 2017;82:703-712. <https://doi.org/10.1016/j.engfailanal.2017.06.001>

Paweł Magryta, MEng. – Faculty of Mechanical Engineering, Lublin University of Technology, Poland.
e-mail: p.magryta@pollub.pl



Konrad Pietrykowski, DSc., DEng. – Faculty of Mechanical Engineering, Lublin University of Technology, Poland.
e-mail: k.pietrykowski@pollub.pl

